Geochemistry Geophysics Geosystems G3

AN ELECTRONIC JOURNAL OF THE EARTH SCIENCES

Published by AGU and the Geochemical Society

Article

Volume 8, Number 10

4 October 2007

Q10001, doi:10.1029/2007GC001644

ISSN: 1525-2027

Measurements of ^{220}Rn and ^{222}Rn and CO_2 emissions in soil and fumarole gases on Mt. Etna volcano (Italy): Implications for gas transport and shallow ground fracture

S. Giammanco

Istituto Nazionale di Geofisica e Vulcanologia, Sezione di Catania, Piazza Roma 2, I-95123, Catania, Italy (giammanco@ct.ingv.it)

K. W. W. Sims

Department of Geology and Geophysics, Woods Hole Oceanographic Institution, Woods Hole, Massachusetts 02543, USA

M. Neri

Istituto Nazionale di Geofisica e Vulcanologia, Sezione di Catania, Piazza Roma 2, I-95123, Catania, Italy

[1] Measurements of ^{220}Rn and ^{222}Rn activity and of CO_2 flux in soil and fumaroles were carried out on Mount Etna volcano in 2005–2006, both in its summit area and along active faults on its flanks. We observe an empirical relationship between (^{220}Rn/^{222}Rn) and CO_2 efflux. The higher the flux of CO_2, the lower the ratio between ^{220}Rn and ^{222}Rn. Deep sources of gas are characterized by high ^{222}Rn activity and high CO_2 efflux, whereas shallow sources are indicated by high ^{220}Rn activity and relatively low CO_2 efflux. Excess ^{220}Rn highlights sites of ongoing shallow rock fracturing that could be affected by collapse, as in the case of the rim of an active vent. Depletion both in ^{220}Rn and in CO_2 seems to be representative of residual degassing along recently active eruptive vents.

Components: 7096 words, 7 figures, 1 table.

Keywords: radon; thoron; carbon dioxide; rock stress; gas transport; Mount Etna.

Index Terms: 8430 Volcanology: Volcanic gases; 8410 Volcanology: Geochemical modeling (1009, 3610); 8419 Volcanology: Volcano monitoring (7280).

Received 25 March 2007; **Revised** 25 July 2007; **Accepted** 14 August 2007; **Published** 4 October 2007.

Giammanco, S., K. W. W. Sims, and M. Neri (2007), Measurements of ^{220}Rn and ^{222}Rn and CO_2 emissions in soil and fumarole gases on Mt. Etna volcano (Italy): Implications for gas transport and shallow ground fracture, *Geochem. Geophys. Geosyst.*, *8*, Q10001, doi:10.1029/2007GC001644.

1. Introduction

[2] Measurement of CO_2 and radon emissions on active volcanoes provide a demonstrated geochemical tool to identify and monitor increased magmatic and tectonic activity.

[3] Carbon dioxide is, after water vapor, the most abundant gas dissolved in magma. Because of its low solubility in basaltic melts [*Pan et al.*, 1991], CO_2 is also one of the first volatile components to be released from magma during its migration toward the surface, and is therefore an important indicator of magmatic activity at depth. While CO_2

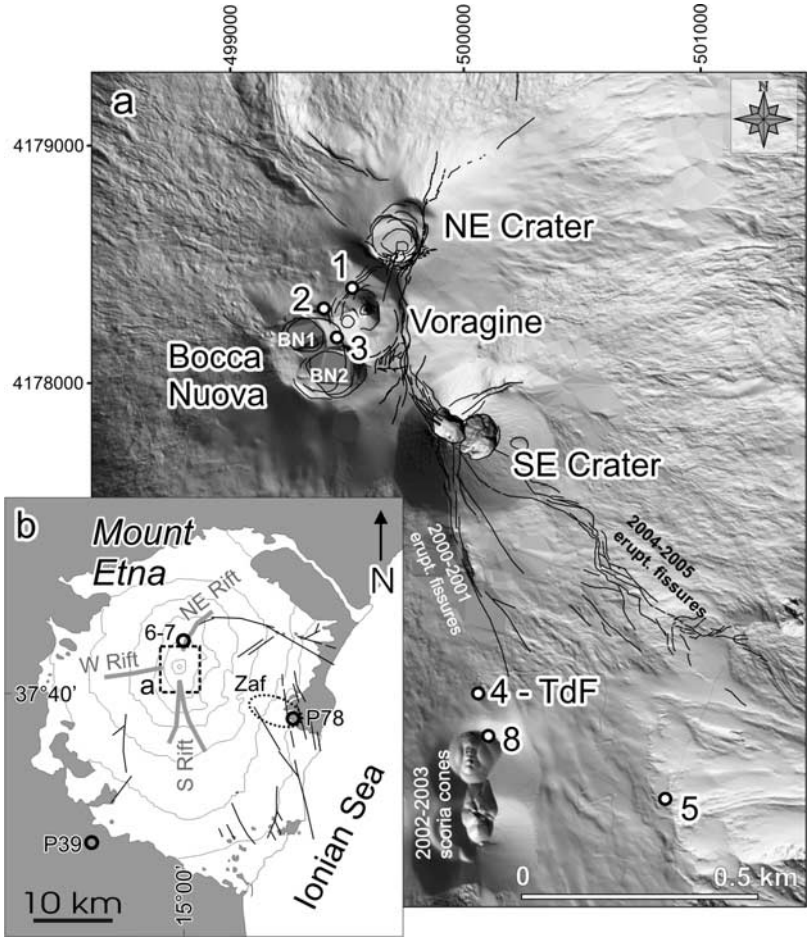

Figure 1. (a) Digital Elevation Model (courtesy of M. Pareschi research group, INGV Pisa) based on 2005 topographic data. Black lines are the main dry and eruptive fracture fields developed in the summit area between 1998 and 2006. Open circles numbered from 1 to 8 represent the locations of the sampled sites in the summit area (higher than 2700 m above sea level). BN1 and BN2 are the two pit craters inside the Bocca Nuova crater. TdF, Torre del Filosofo. (b) Locations of the other sampled points (the open circles indicate sites P39 and P78; the dashed wide circle indicate the Zaf area). Black lines indicate the main faults cutting the volcano; gray lines represent the position of the main rift zones. See text for details.

fluxes are typically greatest from the most magmatically active conduits, significant CO_2 emissions also occur along faults and fissures from the volcanoes flanks [*Allard et al.*, 1991; *Aiuppa et al.*, 2004; *D'Alessandro et al.*, 1997; *Giammanco et al.*, 1995, 1998a, 1998b], and can thus be used to map hidden subsurface faults (i.e., high porosity regions).

[4] Radon is a noble gas and the only naturally occurring radioactive gas. It has three isotopes: ^{222}Rn (radon), ^{220}Rn (thoron), and ^{219}Rn (actinon). Radon is a short-lived decay product derived from the ^{238}U decay series, with a half-life of 3.8 days. Thoron is a decay product derived from the ^{232}Th decay series and has a relatively short half-life (55s) that makes it useful in discriminating sectors with very fast soil-gas transport and/or Th-rich mineral outcrops. Actinon is part of the decay series of ^{235}U and has such a short half-life (4s) that is neglected in geochemical exploration. Although few concurrent measurements of radon and thoron measurements have been previously reported, elevated radon emissions are grossly correlated with high CO_2 emissions; thus ^{222}Rn provides an additional means to identify increased magmatic activity and map active, high porosity regions. In principle, ^{222}Rn, because of its short half-life, has the additional and unique advantage of being able to constrain the timescales of degassing. However, because the main source of the measured radon (shallow soil degassing, deep magma degassing or both) is undetermined, the nature and relevance of the temporal constraints from ^{222}Rn remain uncertain.

[5] To better understand the nature of the processes controlling Rn emissions in volcanic systems we conducted a systematic survey of discrete radon and CO_2 efflux measurements in soil gases at the summit area and flanks of Mount Etna. Measuring CO_2 and both isotopes of radon (^{222}Rn, with $t^{1/2}$ = 3.85 d, and ^{220}Rn, with $t^{1/2}$ = 55 s) from the same samples enables us better constrain the relationship between radon degassing and CO_2 flux and the different half-lives provide important constraints on the source of the radon gas. As we will show, the concurrent measurements of Rn and CO_2 not only provide an important perspective on the timescales of magma degassing, but also provide a means to understand and potentially even forecast the development of important structural changes in an active volcano.

2. Background

2.1. Recent Structural Evolution of Mount Etna

[6] Volcanoes undergo frequent and intense changes in morphology due to the constructive/destructive processes associated with magmatism and tectonism. Mount Etna (Italy) is one of the best examples of a volcano that has been rapidly changing its summit morphology [*Behncke et al.*, 2004]. The present-day summit region is composed of a main central crater named Voragine (VOR), surrounded by three younger near-continuous active craters (North-East Crater or NEC, Bocca Nuova or BN, South-East Crater or SEC), formed in 1911, 1968 and 1971, respectively [*Chester et al.*, 1985] (Figure 1). The volcano also has three fracture zones of volcanic rifting [*Acocella and Neri*, 2003, and references therein], converging toward the summit area: the NE, S and W Rifts (Figure 1b). Etna's summit area is also affected by extensional processes in part related to spreading phenomena that affect the eastern to southwestern flanks of the volcano [*Neri et al.*, 2004, and references therein]. All these processes produce wide fracture fields around and inside the summit craters, recently arranged in a structural system directed approximately N-S (Figure 1) [*Neri and Acocella*, 2006]. In 1998–2001 this system consisted of a N-S fracture zone with orthogonal extension. In 2004 the fractures propagated toward the SE, cutting the SEC and triggering the 2004–2005 eruption [*Burton et al.*, 2005; *Neri and Acocella*, 2006]. On 12 January 2006 an explosive episode occurred at VOR which widely changed the morphology of the summit area. After this activity, the ridge of rock which separated the VOR from the BN was near completely destroyed and the two summit vents today show a common rim which borders a new single and wider crater (Figure 2).

2.2. Previous Measurements of CO_2 and Radon on Mount Etna

[7] As recently known from literature [*Abdoh and Pilkington*, 1989; *Ciotoli et al.*, 1999; *Baubron et al.*, 2002; *Tansi et al.*, 2005], near-surface faults are likely to be sites of high soil degassing and in particular of elevated radon and CO_2 emissions. Consequently, the discrete and/or continuous monitoring of these gases can provide important perspective on the dynamic state of faults [*Burton et al.*, 2004; *Neri et al.*, 2007], as well as providing an indicator of potential eruptive activity [*Alparone et al.*, 2005; *Neri et al.*, 2006].

[8] Etna is an important source of volcanic CO_2 on Earth [*Gerlach*, 1991], even during periods of quiescence. During the last decades many studies have been carried out on Mount Etna regarding both the spatial and the temporal variations of diffuse soil CO_2 emissions, but not as many studies have been carried out on radon emissions (for an extensive review, see *Aiuppa et al.* [2004] and *Burton et al.* [2004]). For the most part, studies on radon were focused on temporal variations of soil ^{222}Rn emissions measured with remote sensors set in a continuous mode [*Badalamenti et al.*, 1994; *Giammanco and Valenza*, 1996; *Alparone et al.*, 2005; *Neri et al.*, 2006]. Only in a very few cases were soil CO_2 and soil ^{222}Rn investigated together, but limited to the spatial variation of their concentrations at 50 cm depth in the ground [*Aubert and Baubron*, 1988; *Badalamenti et al.*, 1994].

[9] Here we describe the importance of concurrent radon and CO_2 flux measurements in both the monitoring the activity of a volcano like Etna, as well as understanding and mapping the development of the important structural and morphological changes.

3. Analytical Methods and Sampling Strategy

3.1. Soil Radon and Thoron Measurements

[10] Soil radon and soil thoron measurements were carried out using a Durridge RAD7 radon meter (http://www.durridge.com/). The RAD7 measures concentrations of both ^{222}Rn (radon) and ^{220}Rn (thoron) in gas phase, by exclusively collecting radon and then counting the alphas emitted by the

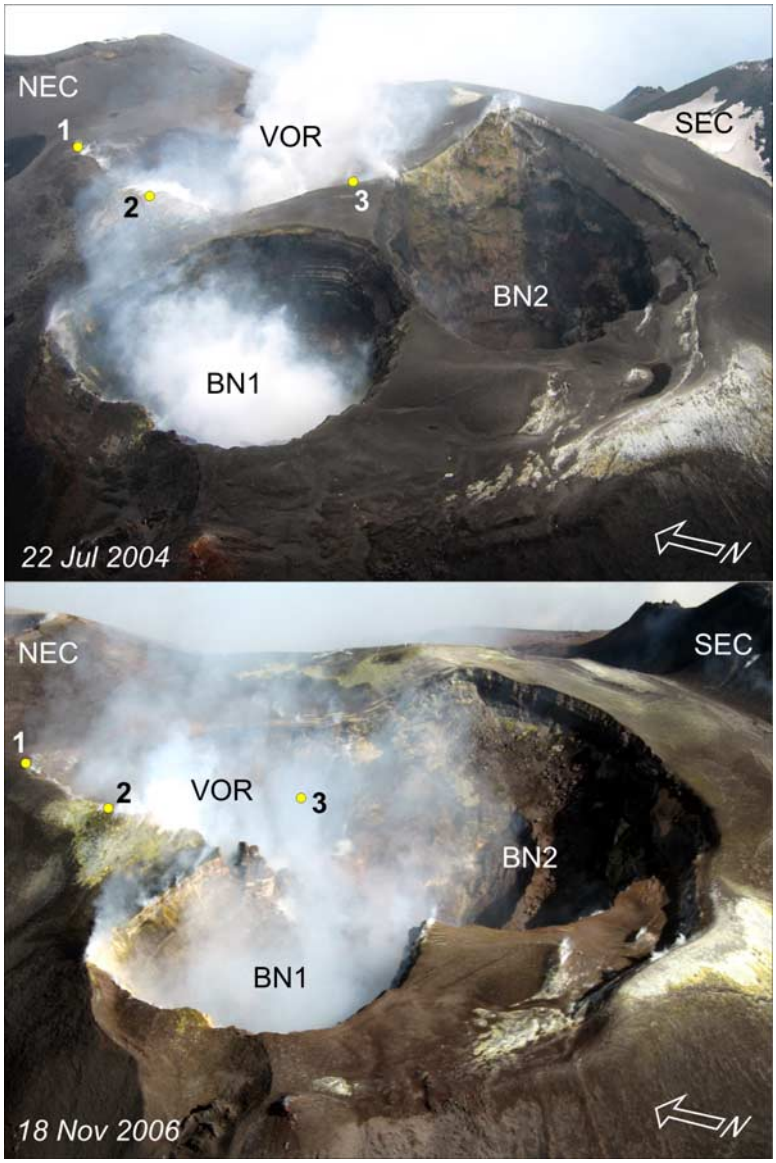

Figure 2. Photos of Bocca Nuova (BN1 and BN2) and Voragine (VOR) summit vents at Mount Etna, (top) before and (bottom) after the 12 January 2006 explosive event. Note the position of site 3, located on the bridge of rocks that separated the two craters before the explosion.

decay of their respective daughter nuclides ^{218}Po ($t^{1/2}$ = 3.04 min) and ^{216}Po ($t^{1/2}$ = 0.145 sec). The soil and fumarole radon and thoron are pumped from the ground at 40 cm depth by an internal pump and their measurement require approximately fifteen minutes pumping in the field, in order to reach equilibrium with the measured daughter nuclide ^{218}Po. The WHOI instruments were calibrated by Durridge prior to each field campaign.

3.2. Soil CO_2 Efflux Measurements

[11] Carbon dioxide effluxes were measured in soil and fumarole emissions using the accumulation chamber method, which consists of measuring the rate of increase of the CO_2 concentration inside a cylindrical chamber opened at its bottom placed on the ground surface. The chamber has an internal fan to achieve an efficient gas mixing and is connected with a portable NDIR (nondispersive infrared) spectrophotometer (PP Systems, UK, mod. EGM4). The change in concentration during the initial measurement is proportional to the efflux of CO_2 [*Tonani and Miele*, 1991; *Chiodini et al.*, 1998]. This is an absolute method that does not require corrections linked to the physical characteristics of the soil. We tested the method in the laboratory with a series of replicate measurements

of CO_2 efflux from a barrel filled with an artificial soil having similar permeability as that of the average soils of Etna; CO_2 was let in through a small pipe at the bottom of the barrel at increasing flows controlled by a digital flowmeter. The average error was about ±5% and the reproducibility in the range 200–1600 g m^{-2} d^{-1} was ±5%.

3.3. Sampling Strategy

[12] A survey of combined discrete field measurements of radon and thoron activities and of CO_2 flux in soil and fumarole gases was carried out on the summit area of Mount Etna in early September 2005. Three sites (numbered 1 to 3 in Figures 1 and 2) were in moderate-temperature fumarolic fields (with significant steam emissions and outlet temperature between about 105°C to 260°C, Table 1) located on the northern and western edges of VOR, on evident fractures running parallel to the outer crater rim. Two sampling sites (4 and 5 in Figure 1) were selected near the summit craters of Mount Etna, in low-temperature fumarolic fields (outlet temperature of about 83°C, Table 1). They were located on fracture fields at Torre del Filosofo (hereafter named TdF; ~2950 m above sea level) and Belvedere. Both of these fracture fields are characterized by fumarolic activity due to boiling of a shallow water table and intense diffuse degassing related to active gas release from the central feeder system of the volcano [*Aubert and Baubron*, 1988; *Pecoraino and Giammanco*, 2005]. Measurements were repeated at site 4 in July 2006.

[13] Last, sites 6, 7 and 8 were located inside some of the eruptive vents that opened during the 2002–03 eruption [*Andronico et al.*, 2005; *Neri et al.*, 2005] both on the northern and the southern upper flanks of Etna (Figure 1); these sites were still emitting steam at the time of sampling.

[14] Eleven more sampling sites were selected on the lower flanks of Mount Etna, in areas characterized by anomalous diffuse emissions of volcanic gas [*Giammanco et al.*, 1995, 1998a, 1998b; *Aiuppa et al.*, 2004; *Pecoraino and Giammanco*, 2005]. Ten of these sites were surveyed in June 2006 in the Etna eastern flank, near the villages of Zafferana Etnea and Santa Venerina ("Zaf" area in Figure 1). One of these sites, namely P78, shows soil CO_2 flux values that are much higher than those of the other sites of this area and are sometimes comparable to those measured at the summit fumaroles. The origin of the gas emitted at this site is magma that accumulates at depths between ~4 and ~10 km along the main feeder system of Etna [*Bruno et al.*, 2001; *Aiuppa et al.*, 2004; *Pecoraino and Giammanco*, 2005]. Within the present study, this site was first measured during the September 2005 survey.

[15] Last, an additional site (P39) was surveyed in July 2006 on the lower SW flank of Mount Etna. This site is characterized by huge diffuse degassing that is produced by a magmatic source located at great depth beneath Mount Etna [*Giammanco et al.*, 1998a; *Caracausi et al.*, 2003; *Pecoraino and Giammanco*, 2005].

4. Results

[16] The results and uncertainties of the geochemical measurements are listed in Table 1. Radon values ranged from 232 to 104,300 Bq m^{-3}, thoron values range from 10 to 23,350 Bq m^{-3}, and CO_2 effluxes ranged from 28 to 26,634 g m^{-2} d^{-1}. Covariance among the measured parameters, both geochemical and environmental (air temperature and pressure, outlet temperature) was evaluated statistically. The most significant correlations were found between CO_2 efflux and outlet temperature values (R = 0.88) and between radon and thoron values (R = 0.66). The former is a typical correlation found in volcanic and geothermal areas [e.g., *Chiodini et al.*, 2005], whereas the latter has previously been observed in other active geodynamical contexts [e.g., *Yang et al.*, 2005].

[17] Plotting radon and thoron data versus CO_2 flux data on a log-log scale (Figure 3), we observe that (1) both ^{222}Rn (Figure 3a) and ^{220}Rn (Figure 3b) activities increase with increasing CO_2 efflux up to about 1000–2000 g m^{-2} d^{-1}, at which point they reach a maximum and decrease with continued increases in CO_2 flux, and (2) the ratio of (^{220}Rn/^{222}Rn) is inversely correlated with CO_2 efflux (R = 0.61), with a few notable exceptions, namely the VOR summit samples and the 2002 vents samples from the NE region. As will also be discussed below, the observation that several samples have (^{220}Rn/^{222}Rn) > 1 has important implications for gas residence and transport times.

4.1. Comparison of Data With a Two-Component Degassing Model

[18] The behavior of CO_2 and radon gases during their transport to the surface can be modeled taking into account the marked difference in the half-lives of the ^{222}Rn and ^{220}Rn.

Table 1. Values of the Parameters Measured in the Sampling Sites at Mount Etna, Divided by Area

Sampling Site[a]	Date of Sampling	Latitude (UTM-ED50)	Longitude (UTM-ED50)	Air Temp., °C	Air Press, mbar	Outlet Temp., °C	CO_2 Efflux, g m^{-2} d^{-1}	^{222}Rn, Bq m^{-3}	Error ^{222}Rn, ±Bq m^{-3}	^{220}Rn, Bq m^{-3}	Error ^{220}Rn, ±Bq m^{-3}	$^{220}Rn/^{222}Rn$
VOR												
1	2/9/2005	499473	4178524	5.1	683	260.0	14,902	2259	1025	3119	1165	1.380
2	2/9/2005	499473	4178524	5.1	683	260.0	26,634	3884	2303	227	14	0.059
3	2/9/2005	499549	4178376	5.1	683	105.0	3705	3271	596	2308	469	0.706
TdF												
4	1/9/2005	500101	4176868	4.7	712	83.8	2440	18,167	15,750	807	10	0.044
4	7/19/2006	500101	4176868	10.0	718	83.1	3712	8770	1175	104	432	0.012
Belvedere												
5	7/24/2006	500932	4176770	7.8	735	82.5	1999	104,300	4775	23,350	3340	0.224
2002–03 Vents												
6	1/9/2005	500809	4181654	8.1	752	87.6	2299	2875	1052	10	10	0.003
7	1/9/2005	500809	4181654	8.1	753	70.5	3170	2013	699	10	10	0.005
8	1/9/2005	500138	4176386	4.5	716	139.2	263	5932	1576	10	10	0.002
E flank												
9	7/6/2006	510196	4173365	23.7	966	22.3	28	320	602	4880	1270	15.250
9	7/14/2006	510196	4173365	28.1	951	27.0	33	232	265	6330	1430	27.284
10	7/6/2006	509909	4173125	22.7	966	20.0	38	3210	749	5210	1310	1.623
10	7/14/2006	509909	4173125	28.0	951	26.4	42	2650	662	4880	1275	1.842
11	7/6/2006	510102	4173272	23.1	966	20.4	36	1560	567	5030	1285	3.224
11	7/14/2006	510102	4173272	28.3	951	26.7	58	2730	673	4510	1230	1.652
12	7/6/2006	510276	4172892	22.8	966	19.0	137	8665	1170	6755	1500	0.780
12	7/14/2006	510276	4172892	28.2	951	27.1	300	8590	1170	6760	1510	0.787
13	7/6/2006	510496	4172925	22.5	966	20.1	111	7840	1125	7975	1625	1.017
13	7/14/2006	510496	4172925	28.1	951	26.9	191	5850	986	10,800	1880	1.846
14	7/6/2006	510583	4172925	22.5	966	20.2	102	8485	1175	11,600	1950	1.367
14	7/14/2006	510583	4172925	28.5	951	27.0	247	5570	965	11,000	1910	1.975
15	7/6/2006	510716	4172692	22.2	966	21.0	69	1864	601	2195	904	1.178
15	7/14/2006	510716	4172692	29.0	951	27.3	77	2630	715	8000	1640	3.042
16	7/6/2006	511816	4172391	22.2	966	20.6	64	9070	1215	8465	1665	0.933
16	7/14/2006	511816	4172391	28.2	951	26.3	161	6900	1080	6320	1480	0.916
17	7/6/2006	510469	4171551	22.2	966	20.0	40	4635	859	4375	1155	0.944
17	7/14/2006	510469	4171551	28.1	951	25.4	56	6930	1000	3610	1170	0.521
P78	1/9/2005	512684	4172212	22.7	978	21.3	2468	24,281	9876	5467	550	0.225
P78	7/6/2006	512684	4172212	25.3	966	24.1	292	29,700	2200	3210	1160	0.108
P78	7/14/2006	512684	4172212	28.1	950	25.0	506	22,000	1890	4320	1290	0.196
SW flank												
P39	7/20/2006	489788	4156007	32.2	1002	21.0	756	8640	1175	1295	794	0.150
Min				5	683	19	28	232	265	10	10	0.002
Max				32	1002	260	26,634	104,300	15,750	23,350	3340	27.284
Mean				20	890	54	2095	10,446	1925	5256	1143	2.235
St. Dev.				9	115	63	5340	18,794	3110	4709	726	5.381

[a] VOR, Voragine vent; TdF, Torre del Filosofo.

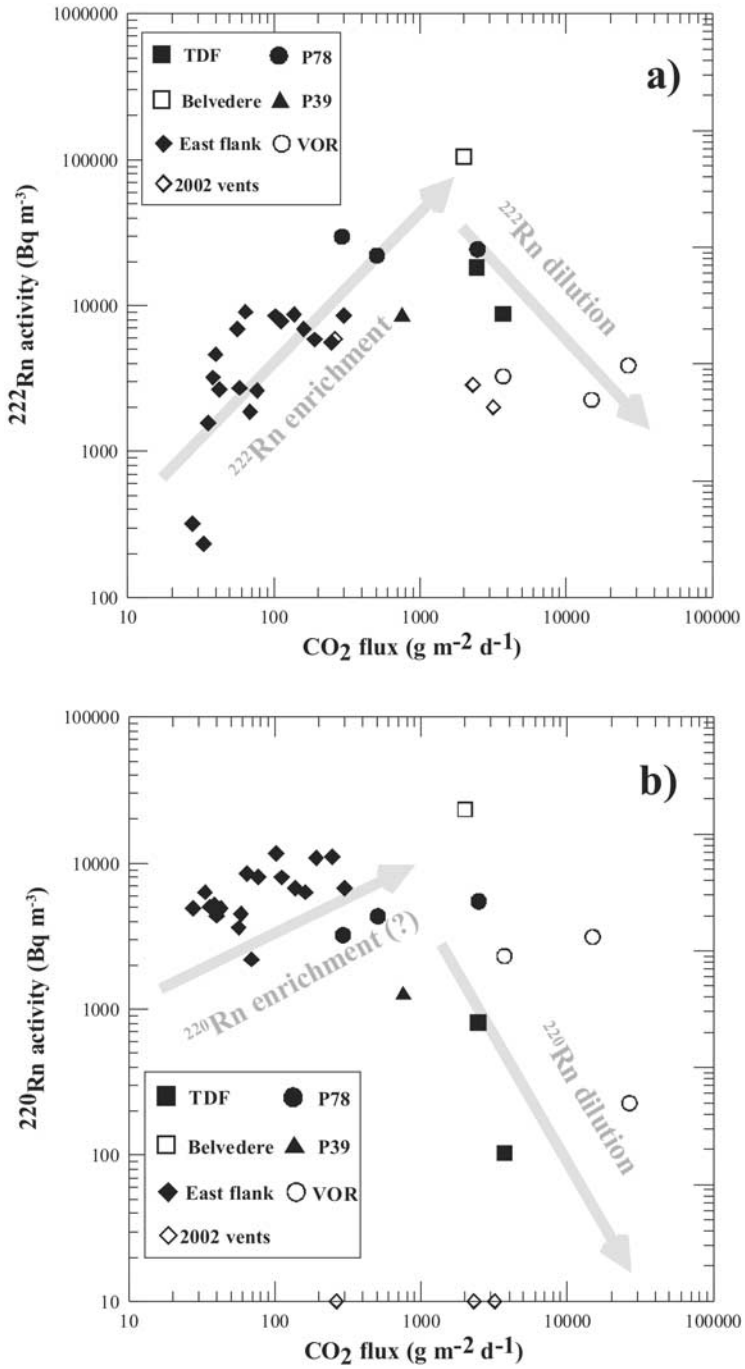

Figure 3. Correlations between (a) (^{222}Rn) "activity" and CO_2 efflux and (b) (^{220}Rn) "activity" and CO_2 efflux measured at all sampling points. Grey arrows indicate the effect of increasing flux of CO_2 as a carrier gas. Assuming CO_2 is the marker of relatively "old" magmatic gas, its increase up to about 2,000 g m^{-2} d^{-1} reduces air contamination (where air is assumed not chemically equilibrated with the soil), thus producing concurrent increases in both ^{222}Rn and ^{220}Rn. This effect is less evident in the case of ^{220}Rn, suggesting that ^{220}Rn has decayed out of the magmatic gas and its inventory is dominated entirely by shallow soil ingrowth and degassing. For values of CO_2 efflux higher than about 2,000 g m^{-2} d^{-1} both radon and thoron decrease and show an inverse correlation with CO_2. This change in behavior is probably due to dilution of both Rn isotopes because the CO_2 flux becomes so high that it overwhelms the shallow source of Rn. The one exception to these trends is represented by the 2002 vent sites, which show very low ^{220}Rn values, as will be shown in detail in Figure 7.

[19] These two isotopes are produced in soils, rocks or magma by alpha recoil input from the decay of the parent nuclides [*Tanner*, 1964; *Krishnaswami et al.*, 1984]. If the source and process producing the measured radon can be determined, then the existence of radon isotopes and their relative abundances place important constraints on the timescales of degassing.

[20] For the purposes of this study, we categorize these different sources of radon as either (1) "deep-magmatic degassing," meaning the radon in the gas is coming from the magma, or (2) "shallow soil degassing," in which it is assumed that the Rn is coming from shallow surficial volcanic rocks and minerals and being carried upward along permeable pathways, such as faults and fractures. In this latter case the "shallow" source is somewhat nebulous. The shallow source composition could be volcanic tephra and lavas, in which case the parental (^{228}Ra/^{226}Ra) will be similar to that of magma, or it could be altered rocks and/or mineral deposits and incrustrations with a variety of different (^{228}Ra/^{222}Ra) activities.

[21] In our modeling we assume that radon degassing is controlled predominantly by advection. Radon's large size and short half-life significantly limit its diffusivity (the length-scale of radon diffusion ranges from a few meters in dry air to about 10 cm in water [*Tanner*, 1964; *Fleischer and Mogro-Campero*, 1978]), and radon's overall low abundances require it to be carried by other gases (e.g., CO_2), whose advective flux is controlled by pressure gradients [e.g., *Shapiro et al.*, 1982; *Toutain et al.*, 1992; *Baubron et al.*, 2002].

[22] The short and markedly different half-lives of ^{222}Rn and ^{220}Rn, relative to the timescales of magmatic (deep) and fumarolic (shallow) degassing, require explicit consideration of supported ingrowth and unsupported decay. In this regard, it is important to note that radon is a noble gas and partitioned into the magmatic gas, whereas its parents and grandparents (Ra, Th, U) are all lithophile and non-volatile and thus preferentially retained in the liquid magma and/or shallow soil. With Rn-ingrowth, if one assumes the Rn in the gas remains in chemical equilibrium with its source then that Rn is considered "supported" and the (^{220}Rn/^{222}Rn) ratio will be determined by the time of ingrowth. This radiogenic process is illustrated in Figure 4a, which shows the ingrowth of both ^{220}Rn and ^{222}Rn and the change in their ratio as a function of time. Because the half-life of ^{220}Rn is much shorter than that of ^{222}Rn, it grows into radioactive equilibrium with its source much sooner, and as a consequence, a "young" gas will have a high (^{220}Rn/^{222}Rn), but low concentrations/activities of (^{220}Rn) and (^{222}Rn). Eventually both (^{220}Rn) and (^{222}Rn) grow into radioactive equilibrium with their supporting parents and the (^{220}Rn/^{222}Rn) activity ratio in the gas approaches (^{228}Ra/^{226}Ra) of the source. Once the gas is no longer in equilibrium with its input source, then the radon isotopes are unsupported and will decay at a rate proportional to their respective half-lives (Figure 4b). Because of the very large difference in their half-lives, ^{220}Rn decays much faster than ^{222}Rn, and the (^{220}Rn/^{222}Rn) becomes diminishingly small in a matter of a few minutes.

[23] In the "deep magmatic gas" end-member case, where it is assumed that the radon budget comes entirely from magmatic degassing, the ^{220}Rn and ^{222}Rn concentrations and (^{220}Rn/^{222}Rn) are a function of the "equilibrium" bubble growth time and the lavas parental (^{228}Ra/^{226}Ra). However, once the bubble escapes or becomes too large to maintain full chemical equilibrium between gas and magma, the (^{220}Rn) and (^{222}Rn) are unsupported and will start to decay according to their respective half-lives. In this simple end-member scenario, measurement of (^{220}Rn) in the gas, because of its 55 second half-life, places strict and rather fast limits on the timescale of gas migration from the magma source to the surface (i.e., <5 min). (^{222}Rn) because of its much longer half-life, will be maintained in the gas for several tens of days. Thus if the magma gas transport time is greater than 5 min, but less than a few days, the magmatic gas will be entirely dominated by ^{222}Rn and the (^{220}Rn/^{222}Rn) will be zero. There are very few constraints on traveltime of magmatic gas after it is exsolved from magma. Studies on magma chambers dynamics and magma residence times on some volcanoes, including Etna, based on (^{210}Pb)-(^{226}Ra) disequilibrium [*Gauthier and Condomines*, 1999] or (^{210}Po)-(^{210}Pb) disequilibrium [*Le Cloarec and Pennisi*, 2001] in crater gases model residence times of gas inside the magma, and assume "instantaneous" times ($\ll$1 day) for ^{222}Rn gas transfer to the surface within volcanic conduits after gas release from the shallow (a few hundred meters deep) magma. Magmatic gas that leaks through the volcano's flanks is certainly slower, both because it comes from a deeper magma and because it travels through rocks with a lower permeability than that of open volcanic conduits, but it is reasonable to infer that it takes some days to reach the surface, and that the ^{220}Rn of the

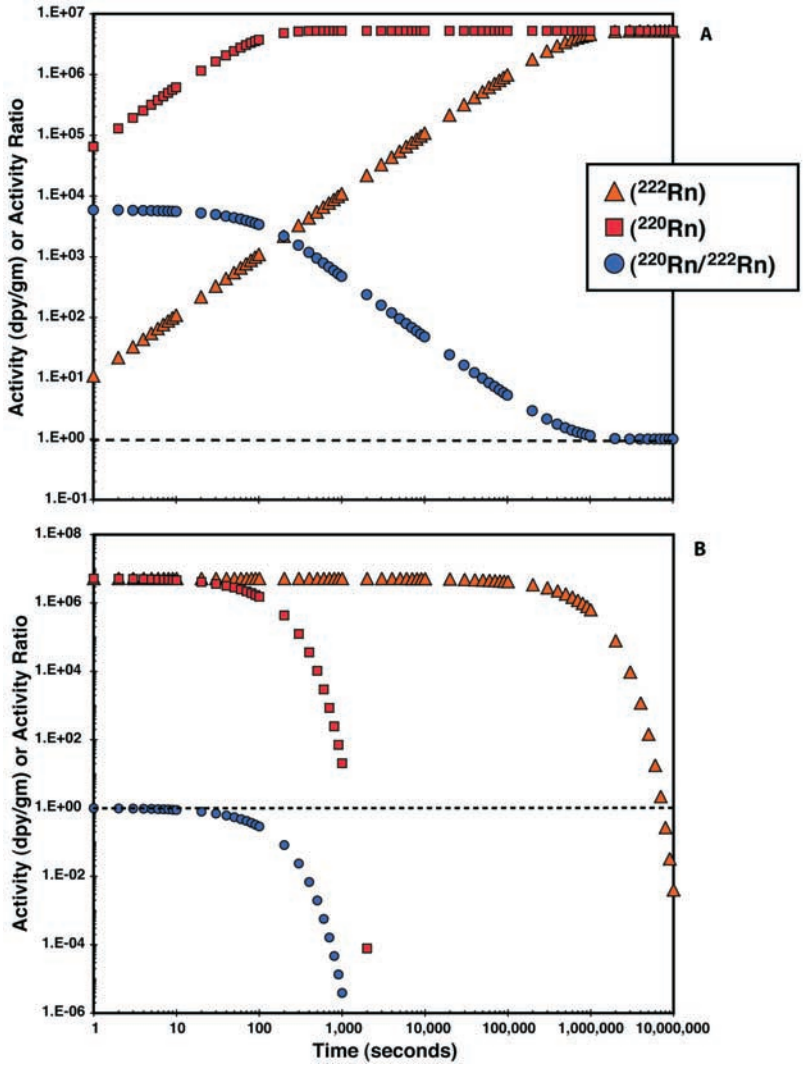

Figure 4. (a) Ingrowth and (b) decay of ^{220}Rn and ^{222}Rn. The ingrowth curve is the development of new gas and can be considered in terms of either magma bubble formation time or soil-gas residence time. Once that gas is no longer in chemical equilibrium with its input source, ^{220}Rn and ^{222}Rn decay at a rate proportional to their respective half-lives.

magmatic gas has entirely decayed and this gas is essentially a ^{222}Rn-dominated CO_2-rich gas.

[24] Alternatively, the radon could be coming from shallow sources, namely "soil and rock degassing" along the porous conduit walls. Since the pathways for gas to travel through rocks and soil are highly irregular, it is likely that the gas stream interacts extensively with the porous wall rocks and that this component contributes significantly to the total radon budget. In this scenario, the measured ^{220}Rn and ^{222}Rn concentrations and ^{220}Rn/^{222}Rn are a function of the parental isotope abundances and the effective residence time of the gas in the "shallow soil" source. In this end-member model, the measured ^{220}Rn constrains the timescale of shallow gas migration to being less than five minutes. This is a more reasonable timescale and is consistent with the findings of *Giammanco et al.* [1998a], who found remarkable air contamination (~95%) in many high degassing sites and even in near-summit fumarole gases with outlet temperature of about 700°C.

[25] The third and most likely possibility is that deep magmatic gases are mixing with gases equilibrated in shallow porous soils. Figures 5 and 6 show a simple model of closed system ingrowth of ^{220}Rn and ^{222}Rn within soil, mixed with a fraction of magmatic ("old") CO_2, containing ^{222}Rn but no ^{220}Rn. The solid curve on the (^{220}Rn/^{222}Rn) versus ingrowth time in Figure 6 shows ingrowth time for

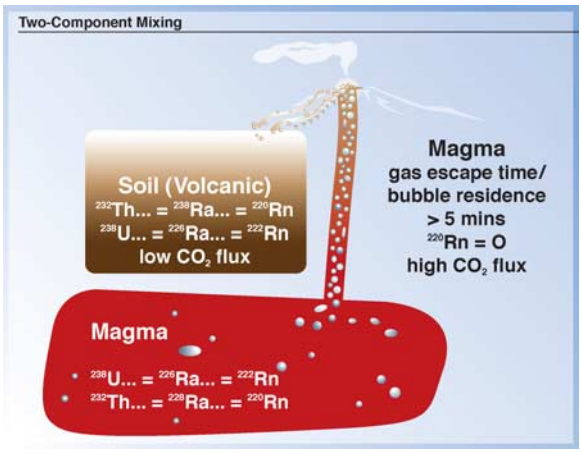

Figure 5. Schematic of closed system ingrowth model of ^{220}Rn and ^{222}Rn within soil, then diluted before analysis with a fraction of "old" CO_2, containing ^{222}Rn but no ^{220}Rn.

the soil since the system was last purged of radon (essentially an approximation to the soil-gas residence time). As the weight fraction of the ^{222}Rn in the system that comes from the "old" component increases the (^{220}Rn/^{222}Rn) ratios decrease. As expected, the lowest (^{220}Rn/^{222}Rn) ratios are seen in systems with the shortest soil-gas recovery time and, presumably, the highest CO_2 flux. In detail, the mixing trajectory expected will depend on the age and origin of the CO_2 (CO_2 exsolved from a ^{226}Ra-rich aquifer could have a much higher (^{222}Rn)/CO_2 than CO_2 exsolved at depth from a magma: potentially explaining why fumarolic emissions may tend to lower (^{220}Rn/^{222}Rn), as seen on Figure 7). The radon isotope systematic can also be considered in terms of the relative flux of ^{222}Rn into the system carried by the "old" CO_2 component. As the ^{222}Rn flux alone is enhanced or diminished (due to changes in the (^{222}Rn)/CO_2 of the carrier gas), the (^{220}Rn/^{222}Rn) ratios will decrease or increase, respectively, following a time-invariant shift. If we assume an increasing flux of magmatic CO_2 into the system, with constant (^{222}Rn)/CO_2, then the expected result is a time-variant shift and the decrease in the (^{220}Rn/^{222}Rn) ratio is accompanied by a fall in soil-gas ingrowth time.

[26] This model is qualitatively consistent with the observed negative correlation between (^{220}Rn/^{222}Rn) ratio and CO_2 flux. Our hypothesis is that this negative correlation represents mixing between

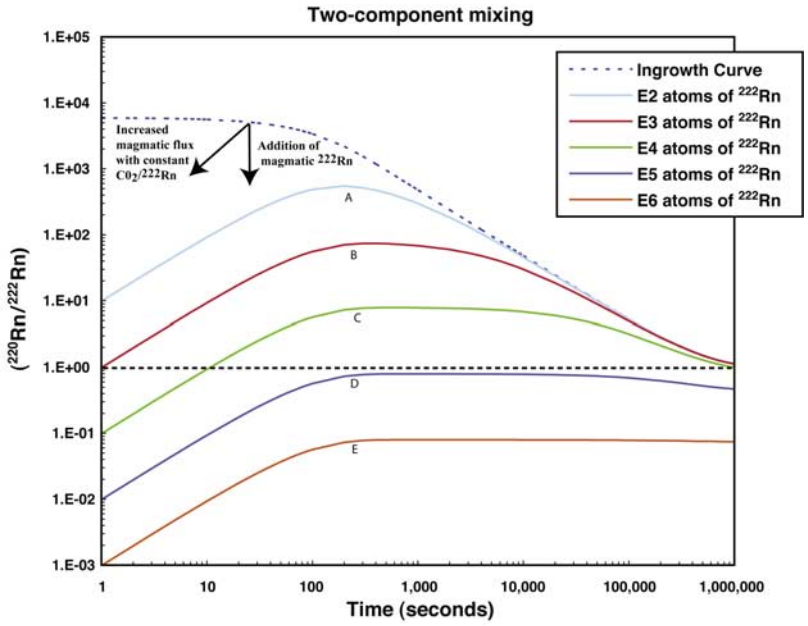

Figure 6. Simple model of closed system ingrowth of ^{220}Rn and ^{222}Rn within soil, then diluted before analysis with a fraction of "old" CO_2, containing ^{222}Rn but no ^{220}Rn. Contours show the proportion (weight fraction) of the ^{222}Rn in the system that comes from the "old" component. The solid line represents soil gas, where the time is the time since the system was last purged of radon (an approximation to the soil-gas residence time). Curves assume that the parental soil activity ratio {(^{228}Ra/^{226}Ra); or (^{232}Th/^{238}U) = 1}. Vertical arrow shows the effect of enhancing the ^{222}Rn "magmatic" flux, due to changes in the ^{222}Rn/CO_2 of the carrier gas. Inclined arrow shows the expected effects of increasing CO_2 flux into the system (assuming that soil-gas ingrowth time falls as a result), with constant ^{222}Rn/CO_2.

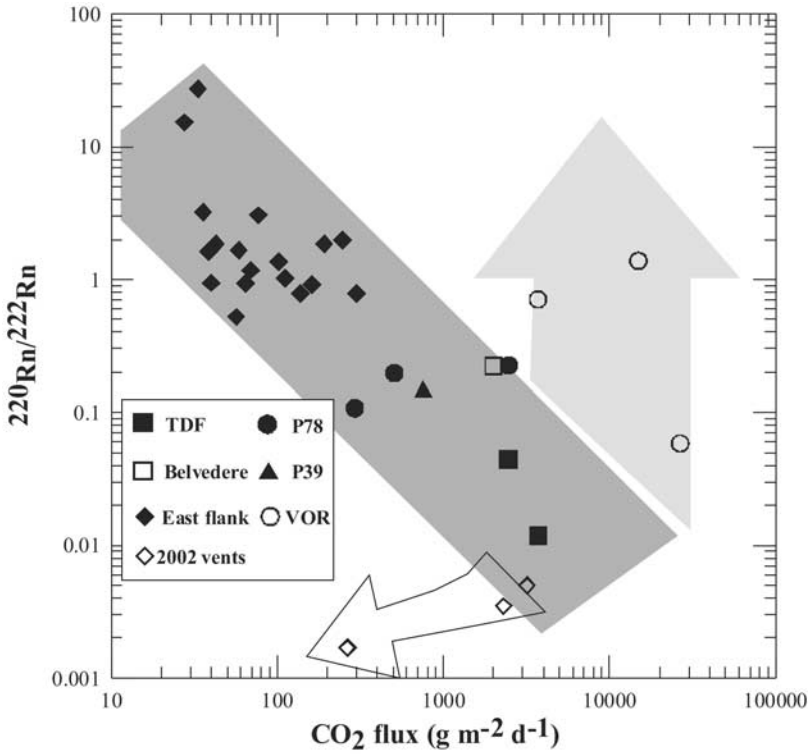

Figure 7. Correlation between the (^{220}Rn/^{222}Rn) and CO_2 efflux in the sampled sites. The dark grey zone indicates the general empirical law that links the studied parameters; the grey arrow indicates sites with excess ^{220}Rn in the gas, due to impending rock fracturing; and the open arrow shows the sites with depletion both in ^{220}Rn and in CO_2, due to residual degassing in recently active eruptive vents.

two end-member components: (1) a shallow soil gas with low CO_2 flux and high (^{220}Rn/^{222}Rn) and (2) a deep, magmatic gas with high CO_2 flux and low (^{220}Rn/^{222}Rn). The shallow degassing component has a high (^{220}Rn/^{222}Rn) as a result of recent ingrowth and short transport times, as the radon is generated near the volcano's surface. The deep magmatic component, on the other hand, is "old" and dominated entirely by ^{222}Rn (as the transport time is greater than 5 min and so the unsupported ^{220}Rn has decayed away entirely). When the flux rate of this deep magmatic component is high, the CO_2 flux increases and the abundance of magmatic ^{222}Rn increases significantly, lowering the (^{220}Rn/^{222}Rn). This increased magmatic gas flux rate has the additional effect of reducing the residence time of the shallow soil gas, this reduced soil residence time serves to even further lower the total contribution of ^{222}Rn and ^{220}Rn from this shallow soil component.

[27] Mount Etna soil and fumarolic gases almost always show an appreciable if not remarkable air contamination [*Giammanco et al.*, 1998a]. If this air contamination is shallow and "young" (i.e., it has not chemically equilibrated with the soil), at modest discharge rates of CO_2, where air contamination is likely to be highest, there will be dilution of the ^{222}Rn (both soil and magmatic) as a result of air mixing. With higher magma gas efflux rates, up to 2000 g m^{-2} d^{-1}, the potential for "air" contamination is substantially reduced and the pressure gradients from the moving gas can draw the degassing radon from a large area in the shallow soils, resulting in the observed relationship between CO_2 efflux and ^{222}Rn concentrations presented in Figure 3a. In the case of ^{220}Rn a similar direct correlation with increasing soil CO_2 effluxes (up to about 2000 g m^{-2} d^{-1}) is not equally evident, suggesting that ^{220}Rn has decayed out of the magmatic gas and its inventory is dominated predominantly, if not entirely, by shallow soil ingrowth and degassing. For values of CO_2 efflux higher than about 2,000 g m^{-2} d^{-1} both ^{222}Rn and ^{220}Rn decrease and show an inverse correlation with CO_2. The most reasonable explanation for this change in behavior is that the flux of the carrier gas (CO_2) becomes so high that it overwhelms the shallow source of Rn isotopes and thus dilutes them both. The one exception to these trends is from the measurements of the 2002 vent sites,

which show very low ^{220}Rn values; these data will be discussed in detail below.

4.2. Evidence for Old Magma and Recent Shallow Faults From Anomalous ^{220}Rn/^{222}Rn

[28] Some sites do not seem to follow the general relationship observed between (^{220}Rn/^{222}Rn) and CO_2 flux showing markedly higher (light grey arrow in Figure 7) or lower (open arrow in Figure 7) (^{220}Rn) activities than the expected behavior. In the latter case, CO_2 efflux values were also lower than expected. It is noteworthy that both of these unique data sets pertain to a well-defined geographic setting. Excess (^{220}Rn) (relative to ^{222}Rn and CO_2 flux) was measured only at the three sites sampled on the VOR crater rim (open circles in Figure 7), whereas depletion in (^{220}Rn) coupled with lower-than-expected CO_2 fluxes was measured only at the 2002 vents (open diamonds in Figure 7).

[29] The higher than expected (^{220}Rn) can be explained by a very shallow source of thoron, which could be ^{232}Th-rich fumarolic incrustations and/or a higher release of ^{220}Rn to the atmosphere because of ongoing rock fracturing near the surface. Although both of these situations may apply in the case of the VOR fumaroles sampled, the latter seems more probable, particularly in view of the recent collapse fractures observed in the ground at all three sites (Figure 2). The structural evolution that the summit area around the VOR and BN craters underwent in the months following our September 2005 survey in the summit area also provides support for this later hypothesis. Similar high (^{220}Rn) emissions relative to ^{222}Rn have been observed in other seismically active areas and have also been explained as microfracturing of shallow rock weeks to months before moderate earthquakes [*Yang et al.*, 2005].

[30] Depletion in ^{220}Rn together with lowering of CO_2 efflux values, as observed in the 2002 vents sites, can be explained by residual degassing from the 2002–2003 magma intrusion that is cooling down inside the eruptive fissures at a depth which is likely to be on the order of hundreds of meters below the surface. In this case, the transport mechanism of gas could approach the ideal case of magmatic gas rising through a conduit with minimal contribution of radon isotopes from the wall rocks, as described above. The 2002 fissure system is actually wide open, thus with a very high ground permeability, but it is structurally stable because no further fracturing occurred after the eruption. Therefore the source of the gases that are convectively released from the 2002 vents, including water vapor, is deep enough and thus old enough to result in complete thoron decay.

[31] Considering the above discussion, the six sites pertaining to VOR and 2002 vents areas deviate from the general observation that (^{220}Rn/^{222}Rn) ratio correlates with CO_2 efflux. When these anomalous data are excluded the observed correlation is greatly improved, with a coefficient R of 0.82 (dark grey area in the plot of Figure 7). On the basis of this general correlation, the TdF site shows the greatest contribution of deep-sourced gas, or the highest velocity of gas. Although sites such as P78 and P39 show geochemical evidence of much deeper sources of gas than that of TdF, as described above, these do not show indication of a very deep origin both of radon and of CO_2. This can be explained considering the interaction between the deep gas and the shallow groundwater table, that is ubiquitous in the Etna area and whose thickness in places reaches several hundreds of meters [e.g., *Aiuppa et al.*, 2004]. Water-gas interaction promotes dissolution of both CO_2 and ^{222}Rn, causing their depletion in the undissolved residual gas phase passing through groundwater. In these cases, the residual gas phase is enriched in ^{220}Rn produced in shallow soil layers above the water table. As a result, sites P78 and P39 (Figure 7) have undergone a shift of values toward a ''shallower'' source of gas.

5. Conclusions

[32] The geochemical survey carried out on Mount Etna shows that independent of the type of gas emission (soil gas, low- or medium-temperature fumarolic gas), the following conclusions can be drawn:

[33] 1. The ''activities'' of (^{220}Rn) and (^{222}Rn) with the soil CO_2 efflux appear to follow a general empirical relationship (Figure 7) that is a function of the mechanism of gas transport toward the surface.

[34] 2. This relationship provides perspective on the type and depth of the gas source, and is more constraining than simply using the ratio between radon and thoron alone.

[35] 3. The state of stress within the shallow rocks near the sampling locations can also be important; rock stress could be induced by a local stress field

related either to the instability of the rim of active volcanic craters, or to an impending earthquake.

[36] 4. Exceptions to the observed empirical relationship between (^{220}Rn/^{222}Rn) versus CO_2 efflux provide information on local conditions such as ongoing rock fracturing (causing thoron excess) or residual degassing from cooling magma intrusions (causing thoron and CO_2 depletion).

[37] 5. Geochemical interactions involving deep ^{222}Rn, and CO_2 and relatively shallow groundwater cause partial dissolution of the deep gases, leading to a more complex interpretation of the data. Other processes occurring at the fumarole sites, such as water condensation under sub-boiling conditions, may cause partial radon and CO_2 dissolution in condensates. However, all of these effects apparently do not significantly alter the information given by the inter-correlation among the studied parameters, namely the relative depth of the gas source and level of local rock stress.

[38] The characterization of gases based on ^{220}Rn, ^{222}Rn and soil CO_2 flux shown in the present work therefore could be considered as an absolute method, at least for Mount Etna, and could be easily applied to other areas of this volcano where anomalous diffuse degassing occurs along active faults that could produce earthquakes with ground fracturing. A similar approach is going to be tested also in other active volcanoes such as Stromboli and Vulcano islands (southern Italy).

Acknowledgments

[39] This work was funded by the Istituto Nazionale di Geofisica e Vulcanologia (S.G., M.N.) and by the Dipartimento per la Protezione Civile (Italy), projects V3_6/28-Etna (M.N.) and V5/08-Diffuse degassing in Italy (S.G.), and NSF EAR 063824101 (K.W.W.S.). This work benefited greatly from conversations with D. Pyle, T. Mather, P. Gauthier, and M. Burton. The comments of D. R. Hilton (associate editor), D. M. Thomas, and an anonymous reviewer improved the quality of this manuscript significantly.

References

Abdoh, A., and M. Pilkington (1989), Radon emanation studies of the Ile Bizard Fault, Montreal, *Geoexploration*, *25*, 341–354.

Acocella, V., and M. Neri (2003), What makes flank eruptions? The 2001 Etna eruption and the possible triggering mechanisms, *Bull. Volcanol.*, *65*, 517–529, doi:10.1007/s00445-003-0280-3.

Aiuppa, A., P. Allard, W. D'Alessandro, S. Giammanco, F. Parello, and M. Valenza (2004), Magmatic gas leakage at Mount Etna (Sicily, Italy): Relationships with the volcano-tectonic structures, the hydrological pattern and the eruptive activity, in *Mt. Etna: Volcano Laboratory*, *Geophys. Monogr. Ser.*, vol. 143, edited by S. Calvari et al., pp. 129–145, AGU, Washington, D. C.

Allard, P., et al. (1991), Eruptive and diffuse emissions of CO_2 from Mount Etna, *Nature*, *351*, 387–391.

Alparone, S., B. Behncke, S. Giammanco, M. Neri, and E. Privitera (2005), Paroxysmal summit activity at Mt. Etna (Italy) monitored through continuous soil radon measurements, *Geophys. Res. Lett.*, *32*, L16307, doi:10.1029/2005GL023352.

Andronico, D., et al. (2005), A multi-disciplinary study of the 2002–03 Etna eruption: Insights for a complex plumbing system, *Bull. Volcanol.*, *67*, 314–330, doi:10.1007/s00445-004-0372-8.

Aubert, M., and J.-C. Baubron (1988), Identification of a hidden thermal fissure in a volcanic terrain using a combination of hydrothermal convection indicators and soil-atmosphere analysis, *J. Volcanol. Geotherm. Res.*, *35*, 217–225.

Badalamenti, B., et al. (1994), Soil gases investigations during the 1991–92 Etna eruption, *Acta Vulcanol.*, *4*, 135–141.

Baubron, J.-C., A. Rigo, and J.-P. Toutain (2002), Soil gas profiles as a tool to characterise active tectonic areas: the Jaut Pass example (Pyrenees, France), *Earth Planet. Sci. Lett.*, *196*, 69–81.

Behncke, B., M. Neri, and G. Sturiale (2004), Rapid morphological changes at the summit of an active volcano: Reappraisal of the poorly documented 1964 eruption of Mount Etna (Italy), *Geomorphology*, *63*(3–4), 203–218, doi:10.1016/j.geomorph.2004.04.004.

Bruno, N., T. Caltabiano, S. Giammanco, and R. Romano (2001), Degassing of SO_2 and CO_2 at Mount Etna (Sicily) as an indicator of pre-eruptive ascent and shallow emplacement of magma, *J. Volcanol. Geotherm. Res.*, *110*, 137–153.

Burton, M., M. Neri, and D. Condarelli (2004), High spatial resolution radon measurements reveal hidden active faults on Mt. Etna, *Geophys. Res. Lett.*, *31*, L07618, doi:10.1029/2003GL019181.

Burton, M. R., et al. (2005), Etna 2004–2005: An archetype for geodynamically-controlled effusive eruptions, *Geophys. Res. Lett.*, *32*, L09303, doi:10.1029/2005GL022527.

Caracausi, A., R. Favara, S. Giammanco, F. Italiano, A. Paonita, G. Pecoraino, A. Rizzo, and P. M. Nuccio (2003), Mount Etna: Geochemical signals of magma ascent and unusually extensive plumbing system, *Geophys. Res. Lett.*, *30*(2), 1057, doi:10.1029/2002GL015463.

Chester, D. K., A. M. Duncan, J. E. Guest, and C. R. J. Kilburn (1985), *Mount Etna: The Anatomy of a Volcano*, 404 pp., Chapman and Hall, London.

Chiodini, G., R. Cioni, M. Guidi, B. Raco, and L. Marini (1998), Soil CO_2 flux measurements in volcanic and geothermal areas, *Appl. Geochem.*, *13*, 135–148.

Chiodini, G., D. Granieri, R. Avino, S. Caliro, A. Costa, and C. Werner (2005), Carbon dioxide diffuse degassing and estimation of heat release from volcanic and hydrothermal systems*J. Geophys. Res.*, *110*, B08204, doi:10.1029/2004JB003542.

Ciotoli, G., G. Etiope, M. Guerra, and S. Lombardi (1999), The detection of concealed faults in the Ofanto Basin using the correlation between soil-gas fracture surveys, *Tectonophysics*, *301*, 321–332.

D'Alessandro, W., S. Giammanco, F. Parello, and M. Valenza (1997), CO_2 output and $\delta^{13}C$ (CO_2) from Mount Etna as indicators of degassing of shallow asthenosphere, *Bull. Volcanol.*, *58*, 455–458.

Fleischer, R. L., and A. Mogro-Campero (1978), Mapping of integrated radon emanation for detection of long-distance

migration of gases within the Earth: Techniques and principles, *J. Geophys. Res.*, *83*(7), 3539–3549.

Gauthier, P.-J., and M. Condomines (1999), ^{210}Pb-^{226}Ra radioactive disequilibria in recent lavas and radon degassing: Inferences on the magma chamber dynamics at Stromboli and Merapi volcanoes, *Earth Planet. Sci. Lett.*, *172*, 111–126.

Gerlach, T. M. (1991), Etna's greenhouse pump, *Nature*, *315*, 352–353.

Giammanco, S., and M. Valenza (1996), Soil gas radon activity on Mt. Etna, *Acta Vulcanol.*, *8*(2), 222–223.

Giammanco, S., S. Gurrieri, and M. Valenza (1995), Soil CO_2 degassing on Mt. Etna (Sicily) during the period 1989–1993: Discrimination between climatic and volcanic influences, *Bull. Volcanol.*, *57*, 52–60.

Giammanco, S., S. Inguaggiato, and M. Valenza (1998a), Soil and fumarole gases of Mount Etna: Geochemistry and relations with volcanic activity, *J. Volcanol. Geotherm. Res.*, *81*, 297–310.

Giammanco, S., S. Gurrieri, and M. Valenza (1998b), Anomalous soil CO_2 degassing in relation to faults and eruptive fissures on Mount Etna (Sicily, Italy), *Bull. Volcanol.*, *60*, 252–259.

Krishnaswami, S., K. K. Turekian, and J. T. Bennett (1984), The behavior of ^{232}Th and the ^{238}U decay chain nuclides during magma formation and volcanism, *Geochim. Cosmochim. Acta*, *48*, 505–511.

Le Cloarec, M. F., and M. Pennisi (2001), Radionuclides and sulphur content in Mount Etna plume in 1983–1995: New constraints on the magma feeding system, *J. Volcanol. Geotherm. Res.*, *108*, 141–155.

Neri, M., and V. Acocella (2006), The 2004–05 Etna eruption: Implications for flank deformation and structural behaviour of the volcano, *J. Volcanol. Geotherm. Res.*, *158*, 195–206, doi:10.1016/j.jvolgeores.2006.04.022.

Neri, M., V. Acocella, and B. Behncke (2004), The role of the Pernicana Fault System in the spreading of Mount Etna (Italy) during the 2002–2003 eruption, *Bull. Volcanol.*, *66*, 417–430, doi:10.1007/s00445-003-0322-x.

Neri, M., V. Acocella, B. Behncke, V. Maiolino, A. Ursino, and R. Velardita (2005), Contrasting triggering mechanisms of the 2001 and 2002–2003 eruptions of Mount Etna (Italy), *J. Volcanol. Geotherm. Res.*, *144*, 235–255, doi:10.1016/j.jvolgeores.2004.11.025.

Neri, M., B. Behncke, M. Burton, G. Galli, S. Giammanco, E. Pecora, E. Privitera, and D. Reitano (2006), Continuous soil radon monitoring during the July 2006 Etna eruption, *Geophys. Res. Lett.*, *33*, L24316, doi:10.1029/2006GL028394.

Neri, M., F. Guglielmino, and D. Rust (2007), Flank instability on Mount Etna: Radon, radar interferometry, and geodetic data from the southwestern boundary of the unstable sector, *J. Geophys. Res.*, *112*, B04410, doi:10.1029/2006JB004756.

Pan, V., J. R. Holloway, and R. L. Hervig (1991), The pressure and temperature dependence of carbon dioxide solubility in tholeiitic basalt melts, *Geochim. Cosmochim. Acta*, *55*, 1587–1595.

Pecoraino, G., and S. Giammanco (2005), Geochemical characterization and temporal changes in parietal gas emissions at Mt. Etna (Italy) during the period July 2000–July 2003, *Terr. Atmos. Oceangr. Sci.*, *16*(4), 805–841.

Shapiro, M. H., J. D. Melvin, T. A. Tombrello, J. Fong-Liang, L. Gui-Ru, and M. H. Mendenhall (1982), Correlated radon and CO_2 variations near the San Andreas fault, *Geophys. Res. Lett.*, *9*, 503–506.

Tanner, A. B. (1964), Radon migration in the ground: A review, paper presented at Symposium The Natural Radiation Environment, Univ. of Chicago Press, Houston, Tex., 10–13 April.

Tansi, C., A. Tallarico, G. Iovine, M. Folino, G. Gallo, and G. Falcone (2005), Interpretation of radon anomalies in seismotectonic and tectonic-gravitational settings: The southeastern Crati graben (Northern Calabria, Italy), *Tectonophysics*, *396*, 181–193.

Tonani, F., and G. Miele (1991), Methods for measuring flow of carbon dioxide through soils in the volcanic setting, report, Ist. Ann. Glob. Appl. Cons. Naz. Ric., Firenze, Italy.

Toutain, J.-P., J.-C. Baubron, J. Le Bronec, P. Allard, P. Briole, B. Marty, G. Miele, D. Tedesco, and G. Luongo (1992), Continuous monitoring of distal gas emanations at Vulcano, southern Italy, *Bull. Volcanol.*, *54*, 147–155.

Yang, T. F., V. Walia, L. L. Chyi, C. C. Fu, C.-H. Chen, T. K. Liu, S. R. Song, C. Y. Lee, and M. Lee (2005), Variations of soil radon and thoron concentrations in a fault zone and prospective earthquakes in SW Taiwan, *Radiat. Meas.*, *40*, 496–502.